Discrimination of particles in neutron detectors

Author: Marian Gómez Cuenca, mgomezcu10@alumes.ub.edu
Facultat de Física, Universitat de Barcelona, Diagonal 645, 08028 Barcelona, Spain.

Advisor: Alfredo de Blas del Hoyo, alfredo.de.blas@upc.edu
Tutor: Assumpta Parreño García, aparrenog@ub.edu

Abstract: This work experimentally compares two charge preamplifiers used with ^{3}He neutron detectors by means of digital pulse-shape analysis: a commercial Canberra and a prototype designed by the Universitat Politècnica de Catalunya (UPC). Measurements were performed with moderated neutron, gamma, and background sources. A signal-processing algorithm that calculates the rise time was implemented. The Canberra system shows excellent discrimination, with a clear separation in the rise time versus energy plots. The prototype of a UPC requires a complementary method, the use of a cadmium filter, to allow correct neutron discrimination. The normalized pulse shapes confirm the differences in rise time for neutrons, gamma rays and microdischarges. Thus, the results demonstrate that the discrimination based on rise time is effective for both systems.
Keywords: ^{3}He neutron detector, charge preamplifier, rise time, neutron spectrum.
SDGs: Industry, innovation and infrastructure; affordable and clear energy.

I. INTRODUCTION

Helium-3 (^{3}He) neutron detectors are fundamental instruments in nuclear physics and technological applications. Their detection principle is based on the reaction:

$$n + {}^3\text{He} \rightarrow p + t + 764 \text{ keV}, \tag{1}$$

where the proton (p) and tritium (t) produced ionize the detector gas, generating a current pulse that can be amplified and measured. For low-background or high-precision applications, it is crucial to distinguish neutron events from other signals such as gamma radiation, alpha particles or electronic noise. A widely used technique is pulse shape discrimination, which analyses the rise time of the signal [1].

This work presents an experimental characterisation of ^{3}He detectors through the acquisition and digital analysis of real pulses. The main objective is to develop and validate a methodology for discriminating neutron events using only the rise time parameter. Although the literature also considers the fall time through the RMS (Root Mean Square) of the decay of the signal tail, this study focuses on using the rise time as the primary discriminating parameter, taking advantage of the difference in pulse shape generated by neutrons and other types of radiation.

Data acquired with two different preamplifiers from a ^{3}He detector exposed to different sources are presented. An analysis routine has been developed that includes pulse digitization, rise time calculation, and the generation of rise time versus energy plots. These plots allow the definition of cut regions to select neutron events.

II. METHODS

II.A. Experimental Setup and Data Acquisition

A proportional helium-3 detector, model LND 252285, was used. These detectors present two advantages. On the one hand, they have a lower level of radioactive impurities in the cathode material than models with aluminum cathodes, and on the other hand, they exhibit lower sensitivity to gamma radiation features that are essential for pulse shape discrimination [2].

The discrimination technique critically depends on the quality and fidelity of the raw signal provided by the preamplifier. To evaluate how the electronics design affects this discrimination capability, comparative measurements were carried out using two different systems:

- An industry preamplifier (Canberra model 2007).
- A prototype preamplifier designed by the Universitat Politècnica de Catalunya (UPC).

To characterize the response to different types of events, measurements were performed with each preamplifier, using:

1. **Moderated neutron source**: A ^{252}Cf sample with activity $A = 4.8$ kBq. The detector was placed inside a cavity made in a 5 cm thick polyethylene moderator block. The polyethylene moderates fast neutrons toward the thermal/epithermal spectrum, maximizing the capture probability through the reaction in Eq. (1), which has a high cross-section at low energies.
2. **Gamma radiation source**: A ^{137}Cs sample ($A =$ 370 kBq) emitting monoenergetic gamma rays at

662 keV:

$$
\begin{aligned}
{}^{137}_{55}\mathrm{Cs} &\xrightarrow{\beta^-} {}^{137m}_{56}\mathrm{Ba}^* + \bar{\nu}_e, \\
{}^{137m}_{56}\mathrm{Ba}^* &\rightarrow {}^{137}_{56}\mathrm{Ba} + \gamma.
\end{aligned} \tag{2}
$$

Additionally, a **background measurement** was performed without sources in order to quantify the intrinsic contributions of the detector itself (such as alpha decays from the detector walls and possible microdischarges) as well as the environmental background.

The acquisition of the electrical pulses was carried out using a digital oscilloscope, controlled by a Python script using the PyVISA library [3]. This system enabled automated and sequential acquisition of waveforms with fixed parameters.

Approximately, and for each preamplifier, 20000 pulses were acquired with the neutron source, 10000 with the gamma source, and 10000 for the background measurement, ensuring robust statistics for the comparative analysis of pulse shapes. The detector operating voltage was kept constant at 1487 V during all measurements, as specified by the manufacturer for optimal operation of this detector model.

II.B. Pulse Processing

The digitized waveforms were processed sequentially to extract the relevant physical parameters. These signals, however, exhibit high-frequency noise inherent to the acquisition electronics. To minimize its impact on the calculation of sensitive parameters such as the rise time, a Savitzky–Golay digital filter was applied to each waveform [4]. This method performs a least-squares fit of a local polynomial over a window of points, which smooths the signal without significantly altering the peak amplitudes. It was selected after testing several options, as it better preserves the pulse shape characteristics while effectively reducing rapid fluctuations.

On the smoothed signal, the rise time (t_r) was calculated, defined as the time required for the pulse to go from 10% to 50% of its maximum amplitude ($A_{\max}$):

$$
t_r = t(50\% A_{\max}) - t(10\% A_{\max}), \tag{3}
$$

This interval avoids the initial region of the pulse, which is more susceptible to high-frequency noise, as well as the region near the maximum, where the signal shape may be less stable. Thus, the rise time was selected as the main discriminating parameter because of its robustness against variations in the absolute pulse amplitude.

The maximum amplitude $A_{\max}$ of each smoothed pulse is proportional to the energy deposited in the detector. To convert the amplitude values into energy (keV), a calibration was performed using the well-known thermal neutron capture peak in ^{3}He at 764 keV. This energy value was assigned to the amplitude channel where the highest density of events was concentrated in the plots shown in Section II.C.

$$
E\ [\mathrm{keV}] = \left(\frac{764\ \mathrm{keV}}{A_{764}} \right) \cdot A_{\max}, \tag{4}
$$

This linear calibration was applied to all measurements.

II.C. Comparative Analysis

Spectral distribution

The energy spectrum recorded by a ^{3}He detector exposed to a neutron source exhibits a characteristic shape that deviates from the expected monoenergetic peak at 764 keV from the capture reaction. This deviation is mainly due to two phenomena:

1. **Wall effect:** When the proton or the triton produced in the capture collide with the metallic wall of the detector before being fully stopped in the gas, only the fraction of energy deposited in the gas is detected. This generates two steps in the spectrum: an edge at 191 keV, when the triton is stopped in the gas but the proton strikes the wall, and another at 573 keV, when the opposite occurs. The peak at 764 keV appears when both particles deposit their full energy in the gas.

2. **Interactions with gamma radiation:** The sources used, as well as the environmental background, contain gamma components that produce a continuous spectrum at low energies, dominating below 200 keV.

Fig. 1 shows the calibrated spectra of the three sources obtained with the Canberra preamplifier. The neutron absorption peak at 764 keV can be clearly observed, together with the characteristic structure of the wall effect. The spectrum of the ^{137}Cs source shows a low-energy distribution corresponding to Compton and photoelectric interactions of gamma rays with the cathode wall.

The UPC spectrum (Fig. 2) shows the expected structure but with greater overlap between the gamma region and the neutron region, along with more pronounced statistical fluctuations. This indicates poorer energy resolution and added electronic noise in the amplification stage, characteristic of a developing prototype.

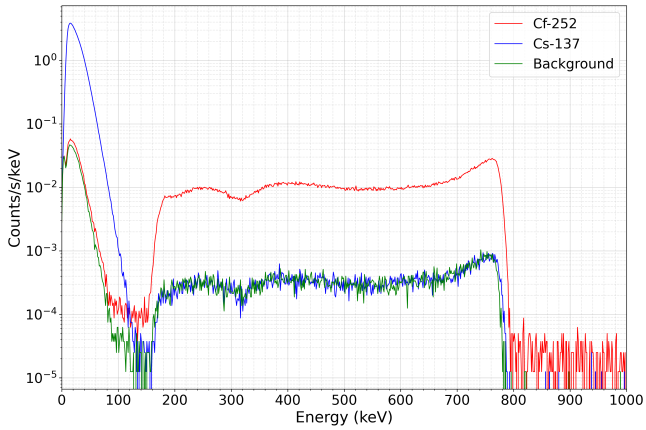

FIG. 1: Calibrated energy spectrum obtained with the Canberra preamplifier. The count rate distribution as a function of energy is shown for the ^{252}Cf (red), ^{137}Cs (blue), and background (green) measurements.

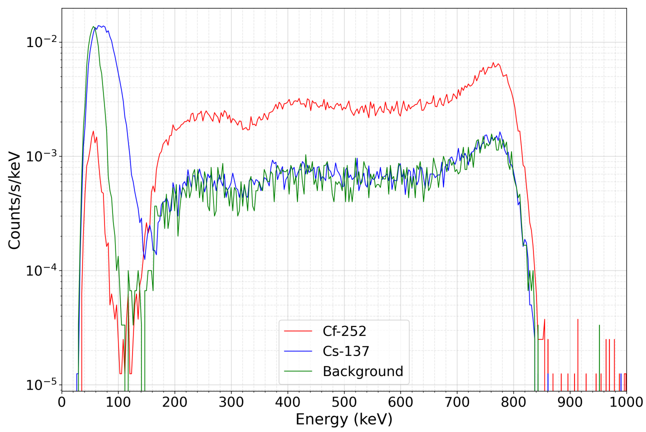

FIG. 2: Same as Fig. 1 but for UPC preamplifier.

The difference between preamplifiers is clear: while the Canberra provides a clean and well-defined spectral response, the UPC introduces electronic noise that dilutes the spectral features. This difference in signal quality will also be reflected in the pulse shape discrimination capability, as shown below.

Rise time as a function of energy diagrams

Using the parameters t_r and energy for each event, two-dimensional histograms (scatter plots) were generated for each source type and preamplifier. These plots are the fundamental tool for visualizing and defining the characteristic regions occupied by neutrons, gamma radiation, and microdischarges.

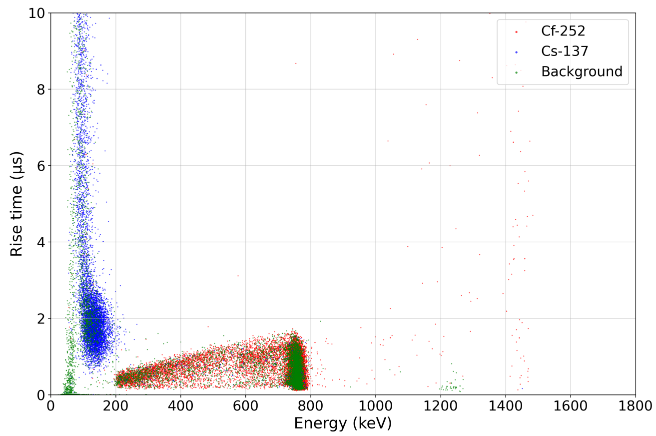

FIG. 3: Rise time as a function of energy for the Canberra preamplifier for the ^{252}Cf (red), ^{137}Cs (blue) sources, and background (green).

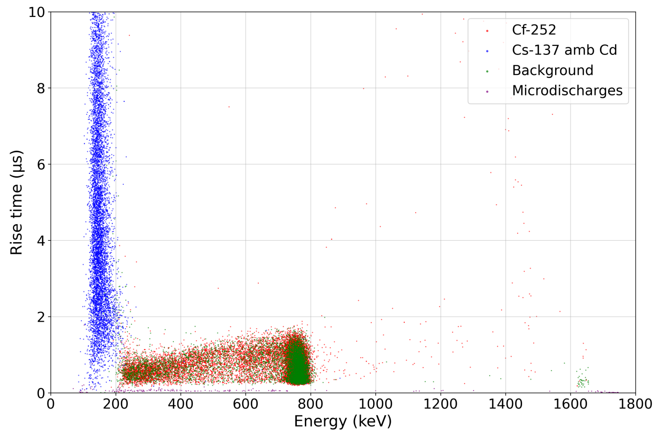

FIG. 4: Rise time as a function of energy for the UPC preamplifier for the ^{252}Cf (red), ^{137}Cs with cadmium filter (blue) sources; and background (green), and microdischarges (purple).

Fig. 3 shows the scatter plot of rise time versus energy for the Canberra preamplifier. Neutrons from the moderated ^{252}Cf source and from the environmental background are concentrated in a well-defined band with rise times between 0.5 and 2 µs and energies around the neutron capture peak (764 keV) as well as the energies covered by the proton and triton wall effect. This clear separation from the gamma rays of the ^{137}Cs source (which appear at energies below 200 keV and with rise times that can reach several µs) allows for defining a trapezoidal cut region that isolates the neutron events. It should be noted that, in this system, the presence of microdischarges is negligible, as expected from a low-noise industrial preamplifier.

In contrast, the same plot for the UPC prototype showed a large dispersion and overlap between neutrons and gammas. To identify the gamma contribution and facilitate the separation, an additional measurement with the ^{137}Cs source was performed, where the detector was shielded with a 1 mm cadmium filter. Cadmium absorbs thermal neutrons, so this configuration allows obtaining the UPC response to gammas only. By superimposing this measurement with that of the moderated ^{252}Cf source and the background measurement (Fig. 4), it is possible to discriminate the neutron event band by exclusion and define a similar cut region.

In this last case, a significant population of events with very short rise times (< 50 ns) distributed across the entire energy spectrum is indeed detected, identified as microdischarges in measurements performed without powering the circuit [5].

II.D. Discrimination Method

Thus, to isolate neutron events in the rise time versus energy plots, a trapezoidal cut region was defined. This region slightly widens as the amplitude (and therefore the energy) increases. It was drawn to cover the area where most points from the neutron source (^{252}Cf) are concentrated, i.e., where the event density is highest. This area also contains points from the other measurements, since the detector always captures some ambient neutrons, while excluding gammas and, in the case of the UPC preamplifier, also microdischarges.

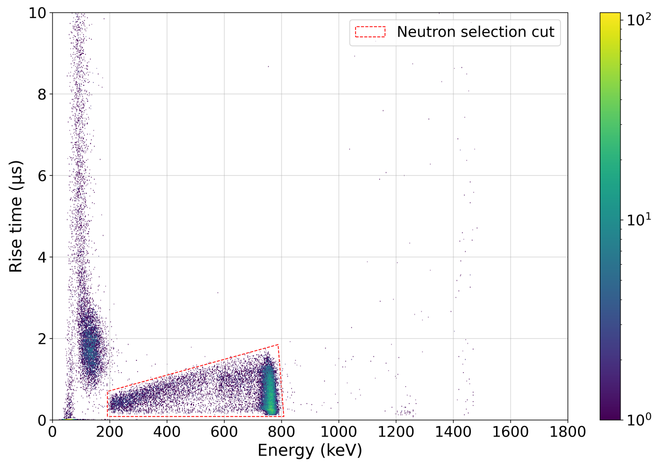

FIG. 5: Rise time as a function of energy for the Canberra preamplifier with the trapezoidal cut region applied (red dashed line). The point density is also shown as a vertical coloured scale on the right.

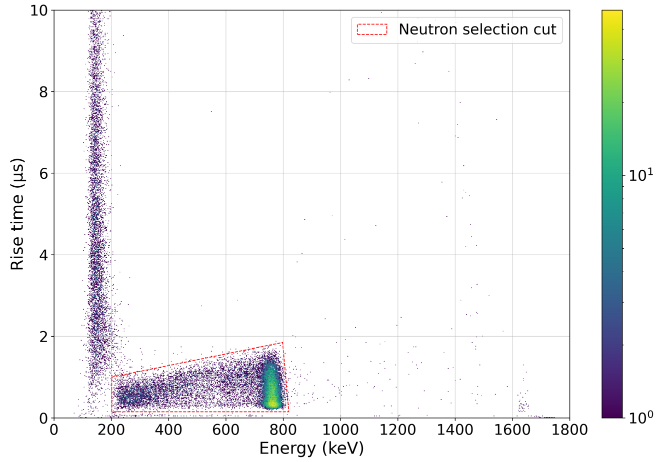

FIG. 6: Same as Fig. 5 but for UPC preamplifier.

To further visualize the physical differences in the response of the two preamplifiers, representative events of each signal type were selected based on the applied cut. Figs. 7 and 8 show the representative traces for neutrons, gammas, and, for the UPC prototype, microdischarges. These traces were amplitude-normalized to highlight the differences in temporal dynamics.

In both systems, the rise time of gamma pulses is significantly longer than that of neutrons, consistent with what is observed in the rise time versus energy plots. It is observed that the UPC exhibits a significantly shorter decay time than the Canberra. Moreover, the intrinsic noise present in the UPC preamplifier may explain the difficulty in performing direct discrimination in the system.

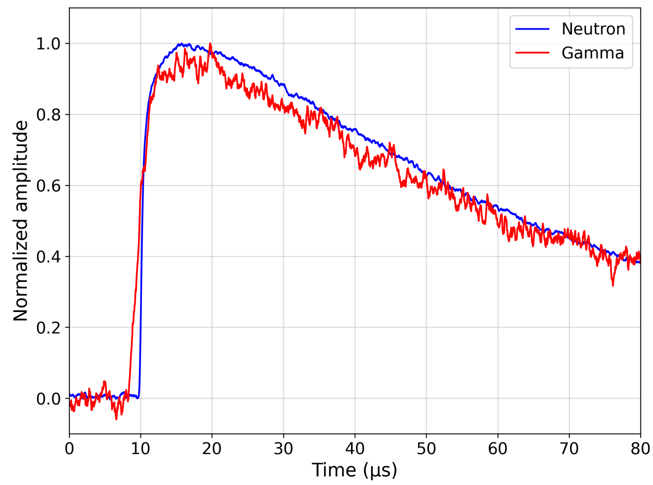

FIG. 7: Normalized pulse shapes for representative neutrons (blue) and gamma radiation (red) acquired with the Canberra preamplifier.

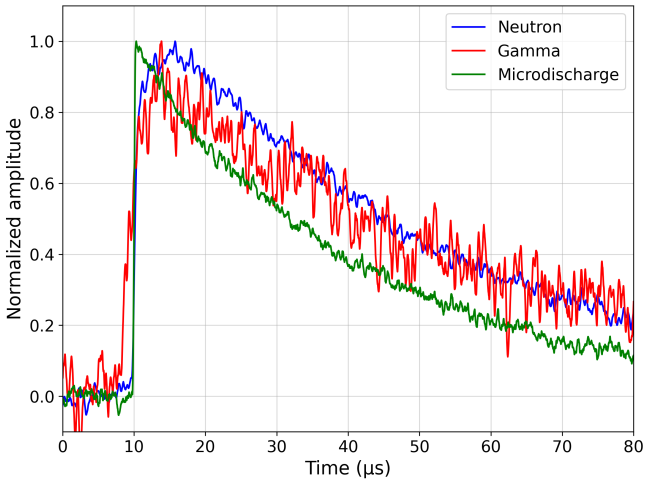

FIG. 8: Normalized pulse shapes for representative neutrons (blue), gamma radiation (red), and microdischarges (green) acquired with the UPC preamplifier.

III. CONCLUSIONS

- The commercial Canberra 2007 preamplifier shows excellent performance for neutron/gamma discrimination using rise time, with well-defined bands and a negligible microdischarge rate, as expected from a commercial low-noise system.
- The UPC prototype is functional and correctly discriminates neutrons when using the cadmium shielding technique, but exhibits characteristics typical of a development-stage design: presence of microdischarges and higher intrinsic noise.
- The normalized pulse shapes confirm the physical origin of the differences in rise time: neutrons produce pulses with intermediate rise times (0.5 to 2 µs), while gammas exhibit longer rise times (up to 10 µs). Microdischarges show very short rise times and extremely fast tails (low RMS).

Acknowledgments

I would like to sincerely thank my external supervisor, Alfredo de Blas del Hoyo, for his trust in me from the very start and for guiding me throughout this project. His insight, encouragement, and unwavering support have been invaluable, and this work would not have been possible without him. I am also grateful to my academic supervisor, Assumpta Parreño, for her guidance and assistance during the development of the project. Special thanks to Eduard Fernández Sadurní for bringing joy and positivity to my days. Finally, I want to express my heartfelt gratitude to my parents, Maria del Carmen Cuenca Aguilar and Jose Luis Gómez Montoya, for their unconditional love and support in every aspect of my life.

[1] T. J. Langford, C. D. Bass, E. J. Beise, H. Breuer, D. K. Erwin, K. M. Heeger, W. Korsch, A. Nucciotti, C. E. Ortiz, and B. L. Goldblum, "Event identification in he-3 proportional counters using risetime discrimination," *Nuclear Instruments and Methods in Physics Research A*, vol. 717, pp. 51–57, 2013.

[2] J. Plaza, T. Martínez, V. Bécares, D. Cano-Ott, D. Villamarín, A. Pérez de Rada, E. Mendoza, V. Pesudo, R. Santorelli, C. Peña, J. Balibrea-Correa, and A. Boeltzig, "Thermal neutron background at laboratorio subterráneo de canfranc," *Astroparticle Physics*, vol. 146, p. 102793, 2023.

[3] PyVISA Contributors, "PyVISA: A Python package for support of the Virtual Instrument Software Architecture (VISA)," May 2023. Software.

[4] A. Savitzky and M. J. E. Golay, "Smoothing and differentiation of data by simplified least squares procedures," *Analytical Chemistry*, vol. 36, no. 8, pp. 1627–1639, 1964.

[5] K. M. Heeger and R. G. H. Robertson, "High-voltage microdischarge in ultra low background ^{3}he proportional counters," *IEEE Transactions on Nuclear Science*, vol. 47, no. 6, pp. 1829–1833, 2000.

Discriminació de partícules en detectors de neutrons

Author: Marian Gómez Cuenca, mgomezcu10@alumes.ub.edu
Facultat de Física, Universitat de Barcelona, Diagonal 645, 08028 Barcelona, Spain.

Advisor: Alfredo de Blas del Hoyo, alfredo.de.blas@upc.edu
Tutor: Assumpta Parreño García, aparrenog@ub.edu

Resum: Aquest treball compara experimentalment dos preamplificadors de càrrega utilitzats amb detectors de neutrons de ^{3}He mitjançant anàlisi digital de la forma del pols: un sistema comercial de Canberra i un prototip dissenyat per la Universitat Politècnica de Catalunya (UPC). Les mesures es van realitzar amb fonts de neutrons moderats, radiació gamma i fons. Es va implementar un algoritme de processament del senyal basat en el càlcul del temps de pujada. El sistema Canberra mostra una excel·lent capacitat de discriminació, amb una clara separació en els diagrames de temps de pujada en funció de l'energia. El prototip de la UPC requereix un mètode complementari, l'ús d'un filtre de cadmi, per permetre una correcta discriminació de neutrons. Les formes normalitzades dels polsos confirmen les diferències en el temps de pujada per a neutrons, radiació gamma i microdescàrregues. Així, els resultats demostren que la discriminació basada en el temps de pujada és efectiva per a ambdós sistemes.
Paraules clau: Detector de neutrons de ^{3}He, preamplificador de càrrega, temps de pujada, espectre de neutrons.
ODSs: Aquest TFG està relacionat amb els Objectius de Desenvolupament Sostenible (SDGs).

Objectius de Desenvolupament Sostenible (ODSs o SDGs)

1. Fi de les desigualtats		10. Reducció de les desigualtats	
2. Fam zero		11. Ciutats i comunitats sostenibles	
3. Salut i benestar		12. Consum i producció responsables	
4. Educació de qualitat		13. Acció climàtica	
5. Igualtat de gènere		14. Vida submarina	
6. Aigua neta i sanejament		15. Vida terrestre	
7. Energia neta i sostenible	X	16. Pau, justícia i institucions sòlides	
8. Treball digne i creixement econòmic		17. Aliança pels objectius	
9. Indústria, innovació, infraestructures	X		

Aquest TFG es relaciona amb l'ODS 9, específicament amb la fita 9.4, perquè contribueix a la modernització i millora de components electrònics per a sistemes de detecció de neutrons, promovent tecnologies més eficients i fiables en infraestructures científiques i industrials. Aquesta millora tecnològica també pot relacionar-se indirectament amb l'ODS 7, fita 7.1, atès que els detectors de neutrons són essencials per al monitoratge i seguretat en instal·lacions energètiques.